

# New Ways of Non-invasive Measuring of Blood Circulation Parameters

KAMIL ŘÍHA<sup>1</sup>, MILAN CHMELAR<sup>2</sup>, RADIM ČÍŽ<sup>1</sup>

<sup>1</sup> Department of Telecommunications  
Brno University of Technology  
Purkyňova 118, 612 00 Brno  
CZECH REPUBLIC  
rihak@feec.vutbr.cz, cizr@feec.vutbr.cz

<sup>2</sup> Department of Biomedical Engineering  
Brno University of Technology  
Kolejní 4, 612 00 Brno  
CZECH REPUBLIC  
chmelar@feec.vutbr.cz

**Abstract:** - The purpose of the article is to describe possible ways of non-invasive measuring and analysis of blood circulation parameters. These parameters are very important indicators of various cardiovascular diseases in clinical practice. For this purpose, methods of purely non-invasive analysis are sought. A standard approach is to use an inflatable cuff for blood pressure monitoring and analysis, using different methods of measuring, typically systolic, diastolic, mean and, less commonly, continuous blood pressure values. Inflatable cuff is a device decrementing a patient's comfort, namely by long-time (24 and more hours) monitoring.

In this article, three principles of purely non-invasive (without inflatable cuff) measurement are described together with some experimental results. The first method described is based on a reliable detection of artery sectional area in the video sequence of B-mode ultrasound images using the Lucas-Canade optical flow determination technique. The output of this method is a cardiac cycle curve evoked by artery diameter changes. The second method for indirect representation of blood pressure parameters is based on measuring the pulse wave velocity, using the R-wave of electrocardiogram (ECG) as the reference signal and the photoplethysmographic sensor for the acquisition of the pulse wave at some distance from the heard (e.g. at forefinger). The third considered way is based on the pulse waveform analysis starting from the hypothesis that the shape of the wave depends on the value of blood pressure.

**Key-Words:** - Optical Flow, B-mode Ultrasound Image, Artery Section Area, Pulse Wave Velocity, Electrocardiogram, Photoplethysmogram, Blood Pressure, Cardiac Curve

## 1 Introduction

Correct functioning of the circulatory system is a fundamental requirement for correct functioning of the whole organism. The functionality of this system can be assessed by monitoring a number of its parameters. They include blood pressure and, more recently, also pulse pressure. This pressure can be measured using invasive and non-invasive methods. In non-invasive blood pressure measurement, the auscultation method using mercury sphygmomanometer is considered the standard. The blood flow through the circulatory system is also described by other quantities related with blood circulation (as used for example in [1]).

Blood circulation in arteries is of pulsating character, which is given by the heart function. The systole of the left ventricle causes a pulse wave on the inlet into systemic

circulation, which propagates through the whole arterial system. The artery wall consists of several layers of different stiffness (see Fig. 1). The velocity and shape of pulse wave depend not only on the pressure in artery but also on the mechanical properties of arterial wall.

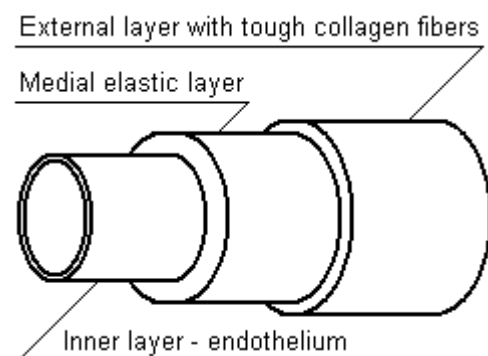


Fig. 1 Anatomy of the arterial wall

A long-term effort at blood circulatory system analysis led to the development of many techniques, mostly using blood pressure measurement with an inflatable cuff. When analyzing the mutual relationship between the time-variant shape or velocity of the pulse wave and blood pressure in arteries, we must realize that blood vessels are not formed by stiff tubes of constant diameter. In practice, the artery is an elastic tube whose diameter varies in dependence on internal pressure. Based on this fact, we can use some purely non-invasive techniques for the description of artery diameter in time and subsequent analysis of resulting signals.

## 2 Ultrasound method

The first method, sonographic displaying, is used in medical practice more likely for pathology findings in combination of a B-mode sonographic image with a Doppler analysis of blood flow. Unfortunately, the Doppler techniques are not very dependable on exact geometric dimensions of an artery and are very sensitive to the sonographic probe position, orientation, motion, etc. There is a possibility of direct B-mode image processing in order to track artery boundaries [2] and to analyse their changes in time (in a sonographic video sequence). This dependence (of geometric parameters on time or on the frame number in the video sequence) may be used for different analyses, in particular for those related to blood pressure and artery elasticity. Hence, the purpose of our work for the first acquisition technique was the determination of artery section area in the sonographic video sequence, the computation of its area, and plotting into a graph.

There exist some methods proposed by other authors in recent years which extract the artery boundary in different ways. A segmentation process is usually used for this purpose such as the Canny edge detection, wavelet filtering, the watershed or the fuzzy C segmentation methods described in [3] and in follow-up articles. The state-of-the-art methods are in their principle very sensitive to random artery abnormalities. On the other hand, the proposed method takes as a challenge the minimization of these problems and the extraction of cardiac curve from noisy and low quality data.

The main advantages of the method presented consist in the fact that it doesn't need the setting of various parameters. It is almost automatic, highly accurate and reliable for various image qualities. Artery borders are not usually highly perceptible, which makes detection very difficult. Our method does not depend on clearly visible borders, which increases its reliability. It can follow the artery being measured even when the sensor is moving

(which causes global motion in the image).

At the beginning of the development of the algorithm, some properties of the method being sought were determined. The method should be preferably non-parametric, automatic, highly accurate and reliable. At the start of processing, we have to accurately and reliably detect the artery circle in first general frame at first. In so doing, we have to take into account that the artery circle can be situated in any part of the image. Moreover, the image contains different pieces of descriptive information and the region of interest may be different for different source data (see Fig. 2).

For that reason, the method includes the first and only manual step, in which the operating person has to do a simple initialization - denotation of the artery in an image. Some tests of fully automatic detection of the carotid shape in a common source image using the Hough transformation have been done (for example in [4]) but the reliability was not 100 %, which is unacceptable in the practice of carotid shape analysis. Hence, some manual algorithm input is necessary. However, the following process of cardiac cycle determination is then fully automated.



Fig. 2 Raw ultrasound image after acquisition

### 2.1 Methodology

The complete method consists of several consecutive image processing steps. The main idea is to track the movement of tissue near the artery border. This is realized by features localised on the artery edge. These features are selected as distinctive points which are tracked during the whole video sequence. The resulting artery cross-section is determined as an area bounded by them.

### 2.1.1 Initialisation

In the first step, some suitable features have to be selected, so that the artery edge can be tracked. This is done by finding the most distinct corners in the image. The positions of found features are sufficiently spaced from each other by choosing the most distinct corners and checking that the distance from the actually selected feature to the nearest next feature is larger than the given minimal distance. This procedure ensures a uniform distribution of selected features in the defined area.

This initialization should be done (with a view to the next processing steps) in the first frame of the video sequence. The proposed procedure is semi-automatic (as mentioned in chapter 1), which means that some area has to be manually denoted for the detection of features. The area has to definitely include an artery border. The suitable shape for such an area has been found in a ring of variable diameter and fixed border width. An example of the initialization step can be seen in Fig. 3.

The above-mentioned ring (defined by the user) can be used as a mask for the method of seeking features for tracking. It is a method implemented in the OpenCV library [5]. The principle of the function is the following.



Fig. 3 Initialization step: the ring-shaped mask for the procedure of finding good features for tracking (a cut-out from source image)

Firstly, the *Hessian*  $H(f(x,y))$  of the image function  $f(x,y)$  has to be computed, which means the matrix of image second derivatives:

$$H(f(x,y)) = \begin{pmatrix} \frac{\partial^2 f}{\partial x^2} & \frac{\partial^2 f}{\partial xy} \\ \frac{\partial^2 f}{\partial yx} & \frac{\partial^2 f}{\partial y^2} \end{pmatrix}. \quad (1)$$

Then a neighbourhood  $S(p)$  of each coordinate in the resulting second derivative functions is included in the calculation. This can be written as

$$M(x,y) = \begin{pmatrix} \sum_{S(p)} \frac{\partial^2 f}{\partial x^2} & \sum_{S(p)} \frac{\partial^2 f}{\partial xy} \\ \sum_{S(p)} \frac{\partial^2 f}{\partial yx} & \sum_{S(p)} \frac{\partial^2 f}{\partial y^2} \end{pmatrix}. \quad (2)$$

Hence, there is a  $2 \times 2$  matrix for every pixel in an image. For this matrix *eigenvalues* are then computed to examine if there is or isn't a corner in terms of the method introduced in [6]. The method denotes a pixel as a corner (good feature to track) if the smaller eigenvalue from two is greater than a fixed given threshold. Thresholded potential corners are then reduced by a further procedure, which removes features accumulated in areas where the Euclidean distance between particular features is smaller than the defined value.

Consequently, the initialization step produces a group of features (their coordinates in an image) under a ring-shaped mask, as can be seen in Fig. 4.

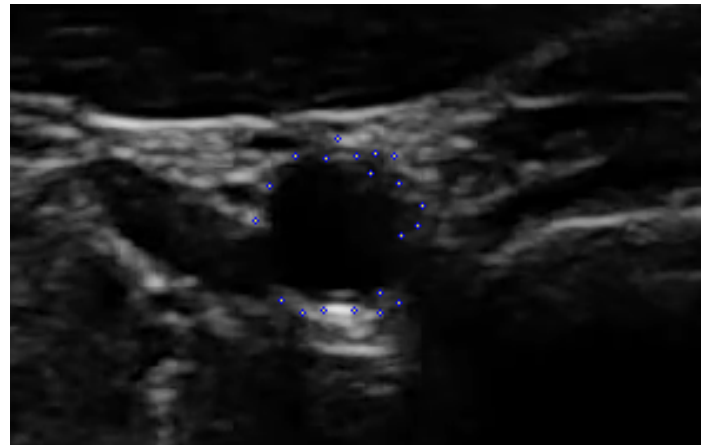


Fig. 4 Detected features denoted in source image after the initialisation procedure

### 2.1.2 Computation of artery section area

During the processing, the artery is represented by a number of features obtained in the initialization step. The features are spread around the artery border, which calls for some fitting function to be used. The shape sought is given by artery cut anatomy and is mostly circular or elliptic (see Fig. 5). Based on the above, the coordinates of features are processed in the least-squares sense and the best-fit ellipse parameters are extrapolated. Based on this, the ellipse area can be computed as the number of pixels in the section area of the approximated artery for every frame in the video sequence analysed.

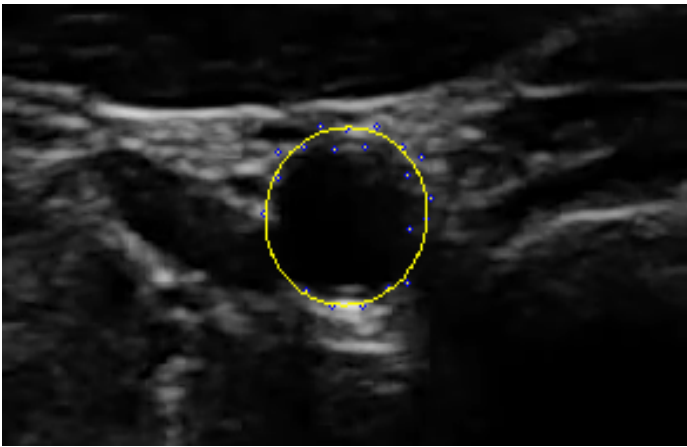


Fig. 5 Ellipse fitted to detected features

The ellipse area can be computed simply by using the equation

$$\text{ellipse area} = \pi \cdot \text{major axis} \cdot \text{minor axis}. \quad (3)$$

Now it is necessary to solve the problem of tracking the features in the whole video sequence. The problem is described in the next chapter.

### 2.1.3 Tracking of features in a video sequence

For tracking the sparse features it is suitable to use the above-mentioned method for optical flow determination by Lucas-Kanade [7]. Its principle consists mainly in the application of the *brightness constancy* assumption

$$E_x u + E_y v + E_t = 0, \quad (4)$$

where  $E(x, y, t)$  is the video sequence,  $E_x = \frac{\partial E}{\partial x}$ ,  $E_y = \frac{\partial E}{\partial y}$ ,  $E_t = \frac{\partial E}{\partial t}$  and  $u = \frac{dx}{dt}$ ,  $v = \frac{dy}{dt}$ . The optical flow vector  $(u, v)$  is sought for every feature and it defines the shift of a given feature pixel  $E(x, y, t)$  in the next image in video sequence (for  $t + 1$  time step). In the equation (4) are two unknowns for one equation and so other equations have to be defined based on the *spatial coherence* assumption, which leads to taking into account  $n$  neighbouring pixels (mostly in a square window). This gives an over-constrained system of linear equations written in the matrix form as

$$\begin{bmatrix} E_{x1} & E_{y1} \\ E_{x2} & E_{y2} \\ \vdots & \vdots \\ E_{xn} & E_{yn} \end{bmatrix} \begin{bmatrix} u \\ v \end{bmatrix} = - \begin{bmatrix} E_{t1} \\ E_{t2} \\ \vdots \\ E_{tn} \end{bmatrix}, \quad (5)$$

which can be solved in the least square sense.

Moreover, the algorithm for optical flow estimation has two improvements in its implementation used from the OpenCv library: iterative scheme for better computational accuracy and pyramidal scheme for better determination of movements larger than the size of analyzed window. These

improvements mainly ensure the stability of tracked points in the sense of following the same part of an image for the whole tracking period. By tracking all the selected points, another important problem is solved, namely that of global motion in the image.

### 2.1.4 Complete scheme of the method

Finally, we can use the processing steps described in the previous chapters and process the whole video sequence as shown by the flow chart in Fig. 6.

The method in the chart tracks the motion of features (optical flow) in the video sequence, fits them to ellipse in every frame, computes the ellipse area and stores the output value also for every frame (area of an ellipse in pixels). This curve (artery section area in dependence on time) is the cardiac cycle with direct relationship to the blood pressure and artery elasticity.

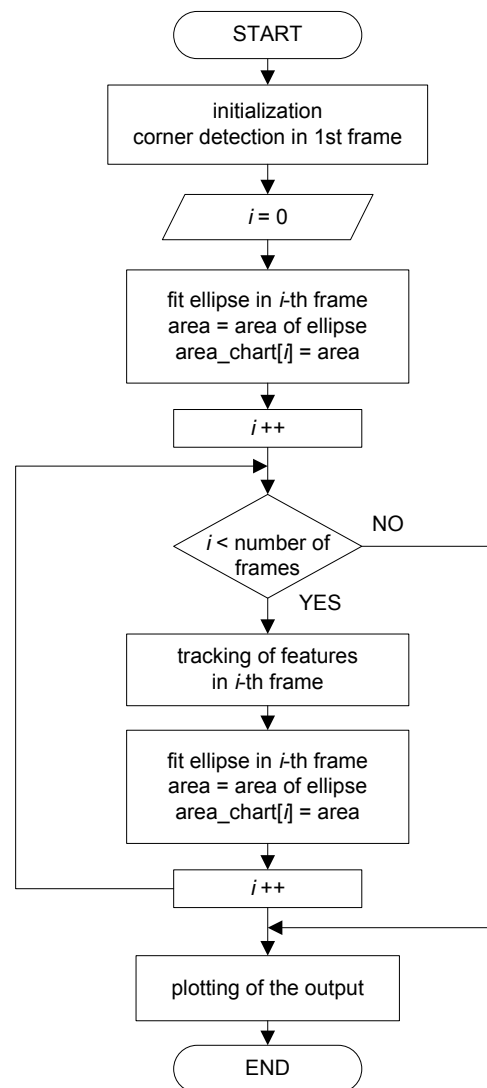


Fig. 6 Flow chart of the method for semi-automatic detection of an artery section area in B-mode ultrasound video sequence

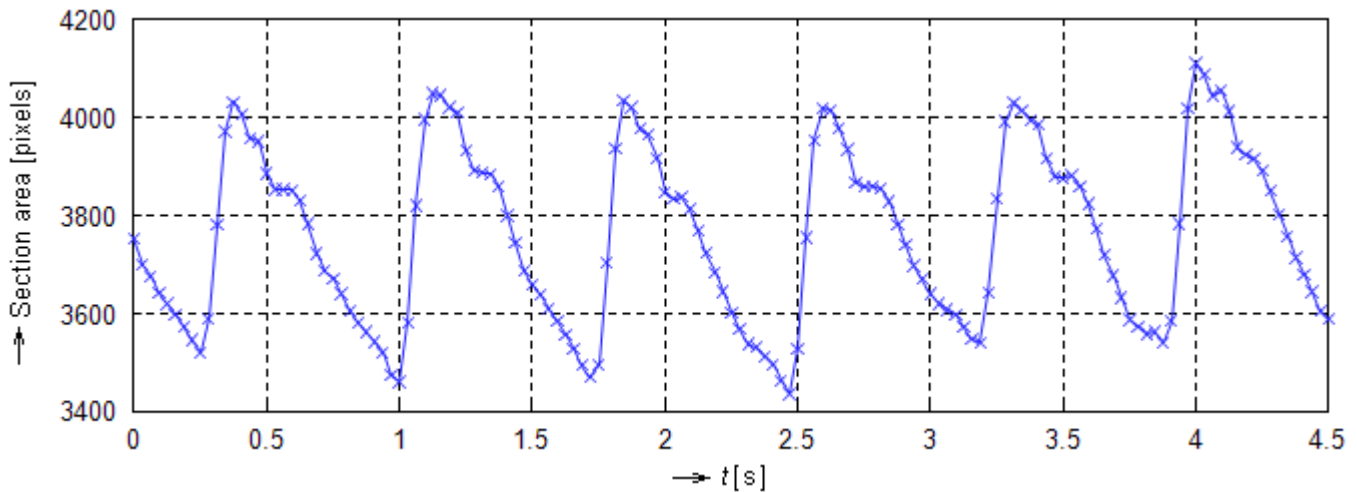


Fig. 7 Final output: the cardiac cycle curve

## 2.2 Experimental results

The output curve is a measure of the quality of processing mainly in the sense of noise appearance. An example of such a typical curve (without any post-processing) acquired by the above method can be seen in Fig. 7. Some other algorithms have been used to solve the problem. Hence, a comparison of their outputs and characteristics is suitable when we are evaluating the quality of the developed method.

In the first place, a very simple method of the so-called *flood filling* can be mentioned. Its simplicity leads to the filled area “escaping” out of the searched inner part of an artery, as can be seen in Fig. 8. The “escapes” can be removed by some post-processing using morphological techniques but there is still a distortion or noise in the output curve.



Fig. 8 Result of simple flood filling algorithm (selected red (bright) area in smoothed image) with clearly perceptible “escape” from the inner part of the artery

The problems with unclear artery borders are partially removed by the complex algorithm [4] using the artificial

immune system method for a decision whether the analyzed pixel is inside or outside of an artery, and the Hough transformation for finding the initial artery circle. Unfortunately, the algorithm is computationally very demanding and the artery circle must pulsate only in one position in the image so that the analyzed area will not “escape” from the initial artery circle. Moreover, many testing video sequences showed that there is often a global artery movement in an image. The presented technique, which is based on the optical flow method, removes problems with both the movement and the unclear artery edges. The results do not contain noise even under strong global motion of the artery circle.

The proposed algorithm has been tested on tens of short sequences, which contained approximately 5 seconds (160 frames), with image/anatomic dynamic information usable for a cardiac cycle curve analysis.

The ultrasound video-sequence was acquired on a *carotis comunis* of an experimental person, using the Sonix OP Smart Ultrasound system with linear probe.

## 3 Pulse wave velocity method

In an artery, the pressure wave which is formed by the left ventricle systole propagates through the arterial system at a velocity that depends on the quality of arterial wall [8]. It was also proved that this velocity depends on the pressure gradient of pulse wave [9]. When we want to compare the pulse wave velocity in different environments, we can choose two cases. The first concerns the propagation of pulse wave through a stiff tube of constant diameter, and the second the propagation of pulse wave through an elastic tubes such as arteries. In a stiff tube filled with incompressible liquid the pulse wave

propagation is infinitely high. When this tube is filled with a common liquid, the velocity may be equal to the sound velocity (c. 1500 m/s in blood). The analysis of the pulse wave velocity in arteries includes many variables such as blood viscosity, elasticity of arterial wall, attenuation of the wave amplitude and the presence of reflected waves due to artery branching. Therefore the real velocity is only 3-12 m/s.

The circulatory system is, in principle, a hydraulic system. Using the analogy between electrical and hydraulic circuits, we can draw the equivalent electrical scheme of a part of artery. The serial RLC circuit, which is an equivalent circuit that describes the properties of a part of artery, is a filter. Its parameters depend linearly on the pressure in the corresponding part of the hydraulic system (i.e. artery). With changes in the parameters of this filter its transfer function also change. This entails a change in not only the pulse shape [10] but also in the delay of this pulse. This means that we can monitor changes in the blood pressure in artery in dependence on the shape or delay of the pulse wave.

### 3.1 Methodology

In connection with measuring the velocity of pulse wave propagation there is a question of which signals could be used for the determination of pulse delay in a given position. One from two possibilities is to compare the ECG signal and the signal of photoplethysmograph [11]. The R-wave peak of ECG, which corresponds to the systole of ventricles, is sharp and therefore it is a suitable reference point. Moreover, the peak on ECG signal can be detected by some automatic method (e.g. [12]). The second possibility is to measure the delay between two corresponding points of two PPG signals obtained by sensors placed on distant positions of the same artery. From the technical point of view, the ECG signal sensing is easy and precise. The problem is, however, that we get exact time of the ventricle systole, but the expulsion of blood from the left ventricle to the artery takes a certain time, which need not be constant. This fact can introduce mistakes in final assessment [13]. Also obtaining of the PPG signal using photoplethysmographic sensor is not difficult, but this method is very sensitive to any movements of the subject scanned.

When we want to relate the pulse wave velocity to changes in blood pressure, we must measure the blood pressure at the same time as the pulse wave velocity. Non-invasive methods for blood pressure measurement are mostly discontinuous so that fast changes in blood pressure cannot be recorded. It is the source of further mistakes in the results of measurement. Only volume-clamp method, invented by prof. J. Peňáz in 1967 and implemented in

Finapres device now, enable non-invasive and continuous blood pressure measurement.

For the measurement of mutual relationship between pulse wave velocity and blood pressure we have used ECG as reference signal, which was detected by electrodes located on the chest of an experimental person. The blood pressure was measured by Finapres and its sensor was placed on the middle finger of the person. The PPG signal was obtained by reflexive photoplethysmographic sensor on the forefinger. The PPG and ECG signals were amplified and together with the signal from Finapres were plugged to the input of data acquisition card PCI-1712 (Advantech) for A/D conversion and further processing by the MATLAB software.

The experimental person was sitting in an armchair, with the left hand placed (together with the sensors) on the arm rest of the armchair and with a weight held in the right hand. We used this isometric loading in order to continually increase blood pressure. Three male persons aged about 30, were the subject of measurement. The block diagram of the experiment is shown in Fig. 9.

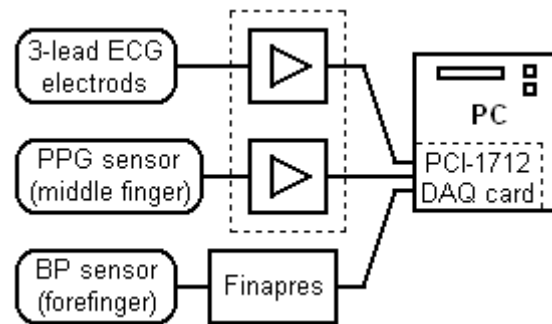


Fig. 9 Arrangement of the measuring equipment

### 3.2 Experimental results

In the first phase of the experiment, the relation between the systolic blood pressure value, which was measured by Finapres, and the reciprocal value of the time delay  $T_1$  between the R-wave of ECG signal and the corresponding peak of PPG signal was sought. The reciprocal value of delay could be simply used instead of pulse wave velocity value because the distance between sensors is constant during whole measurement with an experimental person. It also introduced adequate clarity of the depiction of this dependence in following graphs. For each loading a short section of 3 signals was recorded (see Fig. 10).

Values of systolic (SBP) and diastolic (DBP) blood pressures from Finapres signal were averaged as well as values of  $T_1$  delays which were read from ECG and PPG signals. The results are given in Table 1. They are processed graphically in the next figures.

Table 1 Results

Person	SBP [mmHg]	DBP [mmHg]	1/T <sub>1</sub> [s <sup>-1</sup> ]	1/T <sub>2</sub> [s <sup>-1</sup> ]
No.1	139.5	93.2	3.094	3.378
	141.4	93.1	3.149	3.463
	141.7	92.9	3.210	3.463
	164.3	100.0	3.420	3.723
	169.5	105.0	3.467	3.816
No.2	139.5	88.0	2.931	3.482
	147.7	90.3	3.159	3.695
	162.5	100.0	3.138	3.876
	180.0	110.5	3.121	4.322
No.3	123.5	82.0	2.902	3.035
	128.8	84.5	2.881	3.166
	132.0	87.8	3.002	3.270
	135.0	92.6	3.024	3.321
	135.8	90.3	3.065	3.327

From the results obtained it is clear that there is an evident correlation between systolic blood pressure and pulse wave velocity only for the experimental person No.1 (compare the blue and the green curve in Fig. 11). For the other two persons the results are inconsistent (see Fig. 12 and Fig. 13).

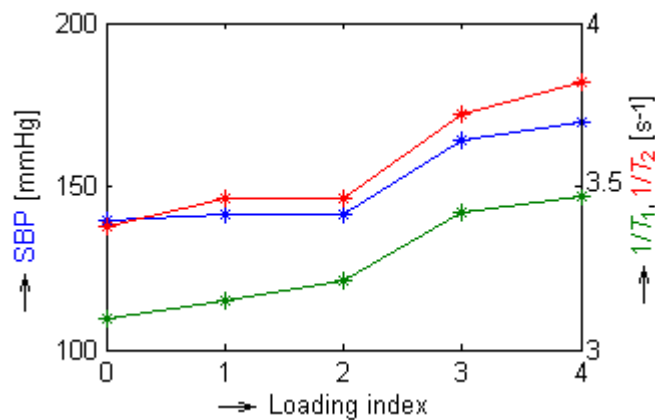


Fig. 11 Progression of values for person No. 1

In an analysis of the obtained results it was discovered that in cases of persons without evident correlation between the blood pressure values and reciprocal values of  $T_1$  delays, there are random phase shifts between PPG and Finapres signal (see  $\Delta T$  differences in Fig. 3). The phase shift was nearly constant in all records acquired during measurement with person No.1. Therefore we carried out yet another assessment. We measured the time delay  $T_2$  between the R-wave of ECG signal and the corresponding peak of the Finapres signal. In this case the relation between  $T_2$  delays and blood pressure values was always in agreement with the assumption that the delay decreases with increasing blood pressure. The better correlation

between blue curve (systolic blood pressure) and red curve ( $1/T_2$ ) is clearly proved in Fig. 11 to 13.

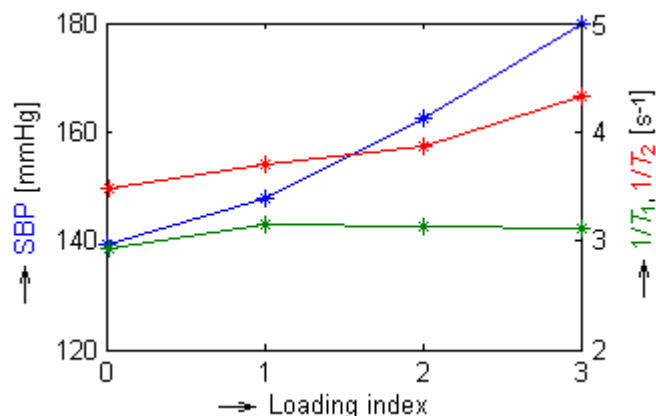


Fig. 12 Progression of values for person No. 2

The problem originates from the location of the photoplethysmographic sensor and the Finapres sensor on the different branches of artery. It disappeared when the place for blood pressure measurement and the place for detection of pulse wave delay were the same.

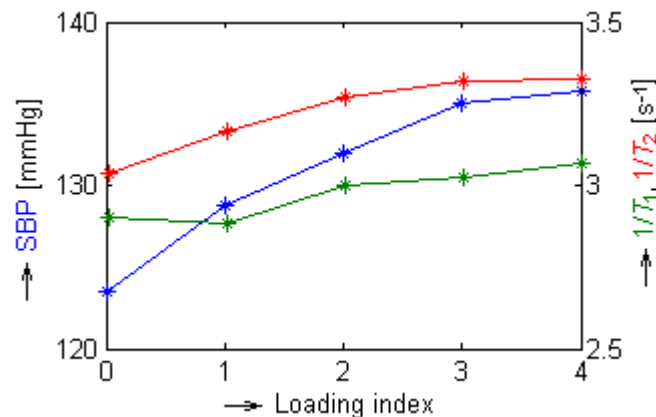


Fig. 13 Progression of values for person No. 3

We suppose these random phase shifts between PPG and Finapres signal are caused by phenomena that occur at points where the artery becomes branched. Blood flowing to the place of branching strikes against the wall between the branches, and these results in turbulence. The turbulence quantity depends on the Reynolds number at the point of artery branching. This turbulence causes a random instability in the distribution of the blood flow into branches [14] and this is reflected in the velocities of pulse wave propagation. In addition, this phenomenon depends on the anatomy of the arterial system of the given person. This may cause significant deviations between signals from Finapres and from the photoplethysmographic sensor. In some cases these difference may be very small, as can be seen from our results for person No.1.

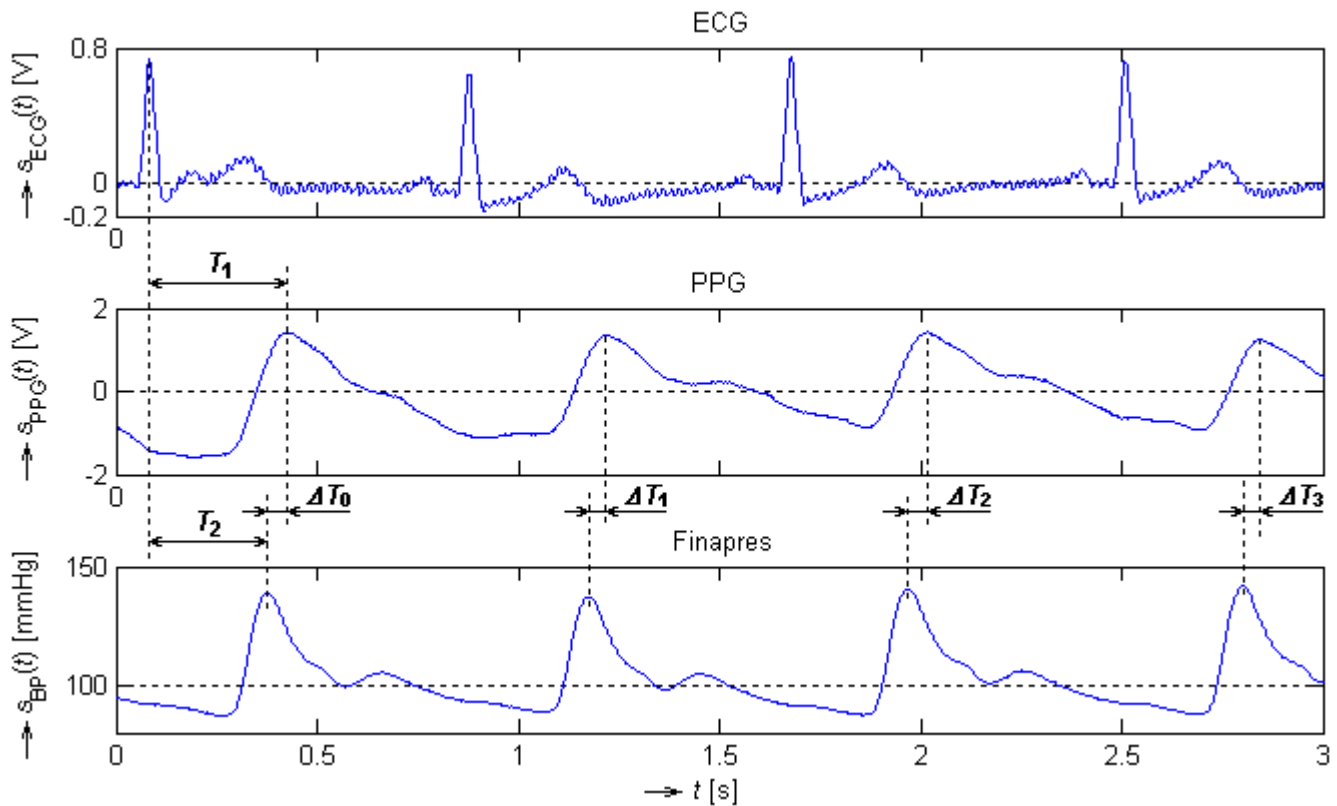


Fig. 10 Recorded signals of person No.2 without loading

### 4 Pulse waveform analysis

As mentioned at the beginning of the previous chapter, in electrical analogy the system of arteries is represented by low-pass filter. Its  $R$ ,  $L$ ,  $C$  parameters depend on voltage, which correspond with blood pressure in the real circulatory system (see Fig. 14).

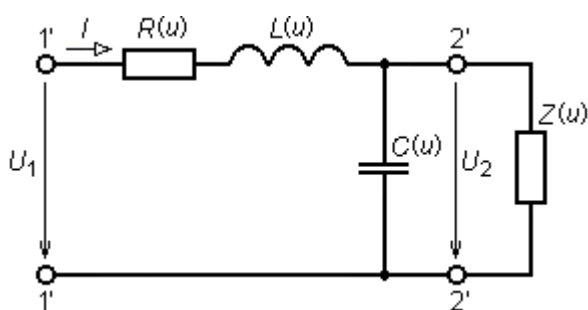


Fig. 14 RLC circuit equivalent to the system of arteries

Transfer function of this circuit is given by relation:

$$H(\omega) = \frac{U_2}{U_1} = \frac{\frac{1}{j\omega C} \parallel Z}{R + j\omega L + \left(\frac{1}{j\omega C} \parallel Z\right)}, \quad (6)$$

which could be modified to the form

$$H(\omega) = \frac{Z}{R + Z - \omega^2 LCZ + j\omega(L + RCZ)}, \quad (7)$$

where

$$Z = \sqrt{\frac{R + j\omega L}{j\omega C}} \text{ is the characteristic impedance.}$$

Increasing blood pressure causes volume increase, thereby the weight of flowing blood also rises, which means an increase of inductance  $L$  in electrical analogy. Reversely, the capacity  $C$ , which corresponds to the stiffness of arterial walls, decreases with increasing blood pressure. These dependence relations are not exactly linear. Resistance  $R$ , which represents the friction coefficient, does not depend on blood pressure too much and it could be regarded as a constant in the typical range of blood pressure values.

The influence of  $L$  and  $C$  parameters on the transfer function of equivalent circuit is depicted in Fig. 15 and Fig. 16. If an increase in the capacity causes the passband reduction, the inductance decrease contrariwise leads to an extension of the passband. In a real circulatory system, a change in blood pressure affects more the weight of

flowing blood then the stiffness of arterial walls. Because of this, the inductance  $L$ , in electrical analogy, could be regarded as a dominant parameter which determines the bandwidth of low-pass filter (see Fig. 15) whereas the opposite influence of the capacity  $C$  could be neglected.

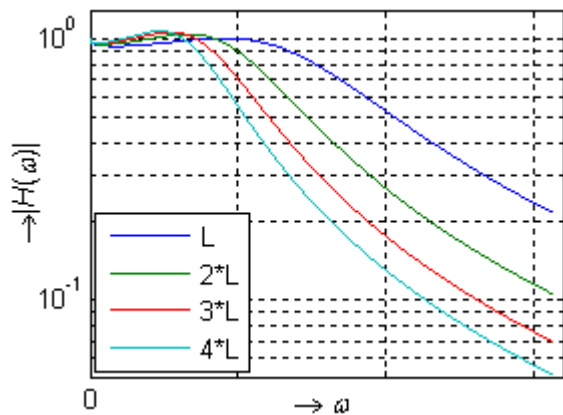


Fig. 15 Influence of increasing inductance

Changing the low-pass bandwidth causes a change in the signal waveform which passes through the filter so that increasing pressure should increasingly suppress the higher harmonic components of the signal, which shows in the reduction of the steepness of the rising and the falling edges of the pulse wave.

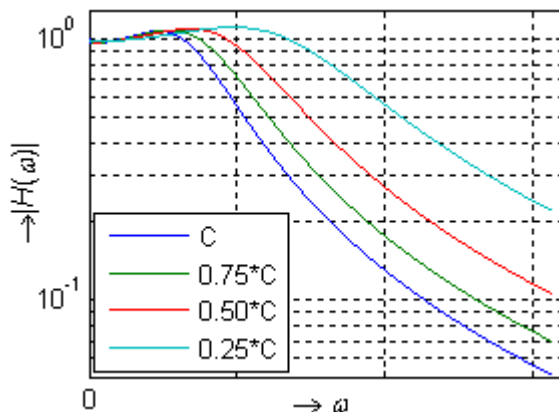


Fig. 16 Influence of decreasing capacity

We tried to prove the above hypothesis, using the harmonic analysis of PPG signals measured on the same experimental person when an isometric loading was increased in order to increase the blood pressure. One typical period was first selected from each signal and consequently resampled so that all waveforms had the same length (see Fig. 17).

Standardization then ensured the same range of values from 0 to 1 of all waveforms, and filtering removed higher-than-10th harmonic components, which belong to noise. After these modifications it was possible to compare the shapes of individual waveforms in Fig. 18.

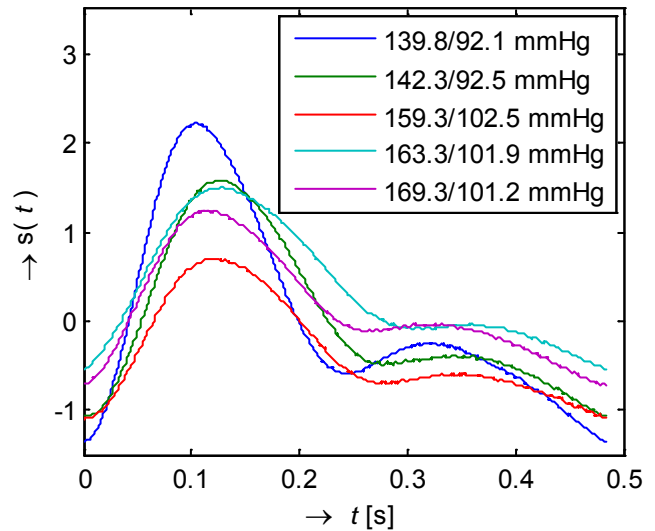


Fig. 17 Resampled PPG waveforms

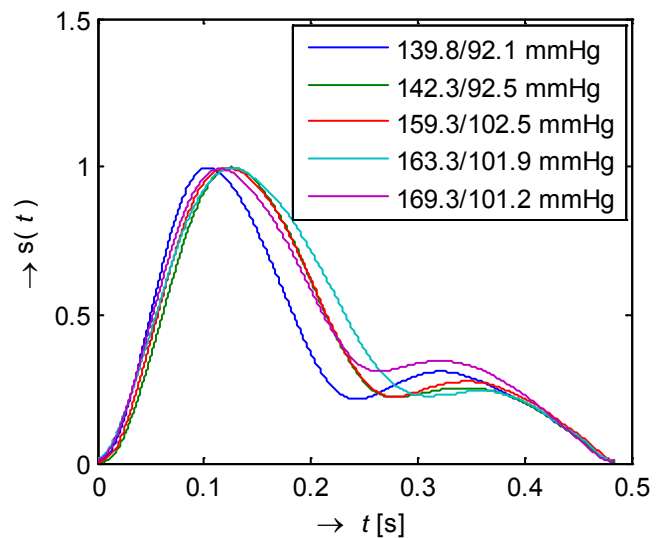


Fig. 18 Standardized and filtered PPG waveforms

The harmonic analysis of modified waveforms was done for the purpose of evaluating the influence of blood pressure on their shapes. In a 3D graph (see Fig.19), the magnitudes of individual harmonic components are depicted for 5 values of blood pressure. Unfortunately, it is not evident from the figure that increasing blood pressure causes a decrease of higher harmonic components.

We believe that signal measuring with a photoplethysmographic sensor is not very suitable for the purpose of subsequent harmonic analysis because the waveforms are greatly affected by the shift of sensor even when the experimental person only slightly moves between two measurements. Because of that, proposed method of pulse waveform analysis seems to be not efficient for non-invasive blood pressure monitoring.

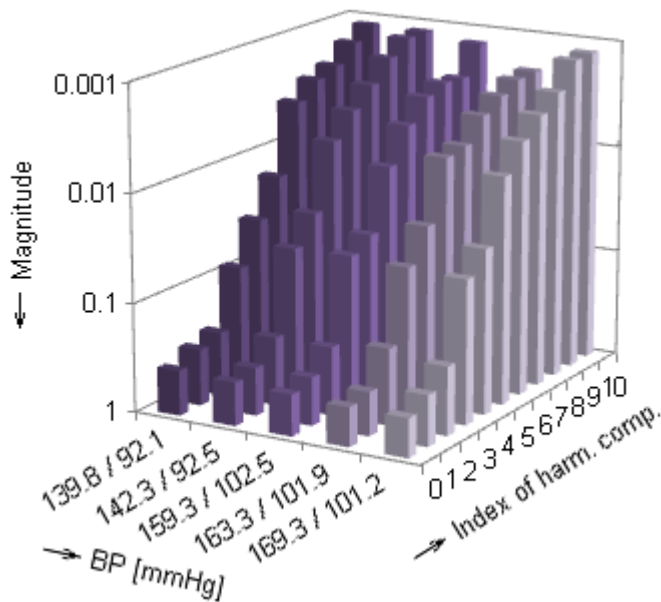


Fig. 19 Harmonic analysis of PPG waveforms

## 5 Conclusion

Three ways of analysing and measuring blood circulation parameters have been presented. Each of these methods produces as an output some information dependent on blood circulation parameters. The proposed techniques have been tested on several experimental persons.

First, a semi-automatic method for cardiac cycle curve extraction from a B-mode ultrasound video sequence using the optical flow technique has been presented. The method produces a curve of artery section area in dependence on time. The curve can be used for a non-invasive analysis the parameters of blood circulatory system. The method needs only one manual initialization step of raw localization of the artery border in the first frame of the analysed video sequence. The tests showed its reliability for various image qualities and sensor motion, and the possibility of processing an image with boundless artery. Using the method is very simple, without any further parameter settings. The utilization of the proposed method can be seen in a wide area of analyses of medical ultrasound video sequences. Physicians can absolutely non-invasively (even without inflatable cuffs) get a cardiac cycle curve (which is proportional to the blood pressure curve) from an arbitrary place in the blood circulatory system.

The second method introduced is a procedure of measuring the pulse wave propagation velocity and its correlation with blood pressure values. A phase shift variation between PPG and Finapres signals within a short period of time has been noticed. It is supposed that the variations are caused by artery branching. An incorrect

placing of PPG and Finapres sensors at the different branches of the artery may cause deviations in the expected correlation between pulse wave velocity and blood pressure. The pulse wave velocity is also influenced by many other quantities [15], which cannot be totally suppressed at the time of measurement. Another question is the reliability of using the ECG as a reference signal. According to some authors [13], the peak of the R-wave is not a reliable reference point for the measurement of pulse wave delay, while it is very suitable from technical point of view.

The pulse waveform analysis was the third method with the lowest potential to be used for a reliable and purely non-invasive description of the correlation between the acquired parameter and the blood pressure. This method has been evaluated as non-perspective because of its high predisposition to a distortion caused by the PPG sensor motion. The distortion has an essential influence on the principal mechanism of the intended method: the amplitude of harmonic components of the signal obtained from the PPG sensor.

### Acknowledgement:

This work was prepared with the support of the Czech Ministry of Education Youth and Sports project No. 2B06111.

### References:

- [1] Jilek, J.; Stork, M. Determination of Blood Pressure and Hemodynamics from Oscillometric Waveforms. In *Proceedings of the 12th WSEAS International Conference on Systems, New Aspects of Systems, PTS I and II*. Heraklion (Greece): WSEAS, 2008. pp. 109-113. ISBN: 978-960-6766-83-1.
- [2] Kubota, R.; Uchino, E.; Suetake, N.; Hashimoto, G.; Hiro, T.; Matsuzaki, M. Genetic Algorithm-based Boundary Extraction of Plaque in Intravascular Ultrasound Image. In *Proceedings of the 7th WSEAS International Conference on System Science and Simulation in Engineering (ICOSSSE '08)*. Venice (Italy): WSEAS, 2008. pp. 91-94. ISBN: 978-960-474-027-7.
- [3] Jayanthi, K. B., Wahida Banu, R. S. D. Carotid Artery Boundary Extraction Using Segmentation Techniques: A Comparative Study. In *Proceedings of the 6th International Conference on Information Technology: New Generations*, Vols 1-3. Las Vegas (Nevada): IEEE, 2009. pp. 1290-1295. ISBN: 978-1-4244-3770-2.

- [4] Řiha, K.; Chen, P.; Fu, D. Detection of Artery Section Area Using Artificial Immune System Algorithm Using Artificial Immune System Algorithm. In *Proceedings of the 7th WSEAS International Conference on Circuits, Systems, Electronics, Control & Signal Processing*. Puerto De La Cruz (Spain): WSEAS, 2008. pp. 46 - 52. ISBN: 978-960-474-035-2.
- [5] Bradski, G.; Kaehler, A. *Learning OpenCV: Computer Vision with the OpenCV Library*. Sebastopol (USA): O'Reilly Media, Inc., 2008. ISBN: 978-0-596-51613-0.
- [6] Shi, J. B.; Tomasi, C. Good features to track. In *Proceedings of the 9th IEEE Conference on Computer Vision and Pattern Recognition*. Seattle (USA): IEEE, 1994. pp. 593-600. ISBN: 0-8186-5825-8.
- [7] Lucas, B. D.; Kanade, T. An iterative image registration technique with an application to stereo vision. In *Proceedings of the 1981 DARPA Imaging Understanding Workshop*. 1981, pp. 121–130.
- [8] Boyd, J.; Buick, J. M. Analysis of changes in velocity profiles in a two dimensional carotid artery geometry in response to resting and exercising velocity waveforms using the Lattice Boltzmann Method. In *Proceedings of the 5th WSEAS International Conference on Fluid Mechanics (FLUIDS '08)*. Acapulco (Mexico): WSEAS, 2008. pp. 41-46. ISBN: 978-960-6766-30-5.
- [9] Xu, Y. Q.; Guan, Q.; Chen, S. Y. Estimation of Dynamic Parameters of Cardiac Ventricles. In *Proceedings of the 10th WSEAS International Conference on Mathematics and Computer Biology and Chemistry (MCBC '09)*. Prague (Czech Republic): WSEAS, 2009. pp. 25-29. ISBN: 978-960-474-062-8
- [10] Padilla, J. M., Berjano, E. J., Sáiz, J., Fácila, L., Díaz, P., Merce, S. Assessment of relationships between blood pressure, pulse wave velocity and digital volume pulse. *Computers in Cardiology*. 2006; 33, pp. 893-896.
- [11] Maguire, M., Ward, T., Markham, C., O'Shea, D., Kevin, L. A comparative study in the use of brachial photoplethysmography and the QRS complex as timing references in determination of pulse transit time, In *Proceedings of the 23rd Annual International Conference of the IEEE Engineering in Medicine and Biology Society*, Turkey, 2001.
- [12] Mohsin, S. Unsupervised Learning based Feature Points Detection in ECG. In *Proceedings of the 8th WSEAS International Conference on Signal, Speech and Image Processing (SSIP '08)*. Santander (Spain): WSEAS, 2008. ISBN: 978-960-474-008-6.
- [13] Payne, R. A., Symeonides, C. N., Webb, D. J., Maxwell, S. R. Pulse transit time measured from the ECG: an unreliable marker of beat-to-beat blood pressure, *J.Appl. Physiol.* 2006, 100: pp. 136-141.
- [14] McDonald, D. A. *Blood flow in arteries*. Southampton (Great Britain): Camelot Press Ltd, 1974, ISBN 0 7131 4213 8.
- [15] Choi, B., Kim, S., Jung, D., Jeon, G. Effect of factitious breathing on pulse transit time and heart rate, *IFBME Proceedings* Vol.14/2.